RJC

RASĀYAN *J. Chem.*
Vol. 18 | No. 3 |1549-1556| July-September | 2025
ISSN: 0974-1496 | e-ISSN: 0976-0083 | CODEN: RJCABP
http://www.rasayanjournal.com
http://www.rasayanjournal.co.in

GREEN SYNTHESIS OF HYBRID SUPERABSORBENT HYDROGELS OF ACRYLIC ACID, MODIFIED VINYLTRIMETHOXYSILANE (VTMS) AND BAGASSE-DERIVED NANOSILICA UNDER LOW-ACID AND HIGH-ACID SORPTION CONDITIONS

P. Susmanto✉, T. I. Sari, N. Haryani, A. Hasanah and L. Khairunnisa
Department of Chemical Engineering, Faculty of Engineering, Universitas Sriwijaya, Jl. Palembang-Prabumulih KM 32 Inderalaya, Sumatera Selatan, Indonesia, 30662
✉Corresponding author: prahady.susmanto@ft.unsri.ac.id

ABSTRACT

This study aims to determine the impact of variations in initiators and cross-linking agents on the absorption capacity, swelling ratio, and characteristics of superabsorbent hydrogels. Superabsorbent hydrogels were synthesised using acrylic acid as the monomer, ammonium persulfate (APS) as the initiator, and Vinyl Silica Nanospheres (VSNPs) as the cross-linking agent, which are modified from Vinyltrimethoxysilane and bagasse nanosilica compounds. Modification of Vinyl Silica Nanospheres (VSNPs) from bagasse silica ash to achieve Sustainable Development Goal (SDG) 13: Climate Action. The production of superabsorbent hydrogels in this study utilised the free radical polymerisation method. Analyses in this study included water absorption analysis, swelling analysis in pH 4 and pH 9.81 solutions, as well as FTIR, XRD, and SEM analyses to determine the characteristics of superabsorbent hydrogels in the best samples. The results showed that the best sample was achieved at a variation of 0.1 grams of initiator and 0.1 grams of crosslinker, with a water absorption capacity of 74,139%. The highest swelling ratio was achieved at pH 9.81, which was 31,317%. The polymerisation results showed absorption peaks at 1,044.31 cm^{-1} and 1,169.82 cm^{-1}, corresponding to the carboxylate functional group (C-O). SEM analysis showed that the hydrogel had a complex structure with long chains, indicating the presence of cross-links between monomers, initiators, and cross-linking agents.

Keywords: Superabsorbent Hydrogel, Nanosilica, Vinyltrimethoxysilane, Sugarcane Bagasse, Polymerization.
RASĀYAN *J. Chem.*, Vol. 18, No.3, 2025

INTRODUCTION

Recently, superabsorbent hydrogels (SAHs) have become one of the main focuses in the world of research. Innovations in the production of superabsorbent hydrogels continue to evolve. The development of SAHs is aimed at achieving the best quality results, being more environmentally friendly, and being naturally biodegradable, thereby contributing to SDG 13 on climate action. One of the key characteristics that SAHs must possess is their ability to absorb and retain a very large amount of water compared to their weight.[1] However, low absorption capacity and swelling remain major issues. Synthesis methods, the use of effective monomers, cross-linking agents, and initiators, as well as the addition of nanoparticles, are some approaches that can be applied to enhance absorption capacity. Modifications in the use of monomers, cross-linking agents, and initiators have been made to produce the highest quality hydrogels. In some studies, modifications to the raw materials used have been reported to increase the water absorption capacity of SAH.[2] When compared to the original acrylic acid nanocomposite hydrogel and the one containing original SiO_2, it was found that the nanocomposite hydrogel containing NH_2-modified nano-SiO_2 had a higher expansion value. The higher development value can increase the absorbency of the hydrogel; therefore, modifying this raw material significantly enhances the performance of the produced hydrogel. Silica nanoparticles have the potential to improve material performance by improving pore structure, increasing the strength and stability of the hydrogel.[3] This study used a formulation of silica nanoparticle material made from sugar bagasse, a natural raw source. Sugar bagasse has a silica concentration of 80%.[4] The silanol group (Si-OH) on silica nanoparticles (SiO_2) has good biocompatibility, homogenous pore size,

http://doi.org/10.31788/RJC.2025.1839307

configurable particle size, large surface area, and is easy to change.[5] Silica nanoparticles derived from bagasse will be modified by adding vinyltrimethoxysilane (VTMS). The modification of these two materials will be used as a crosslinking agent in the synthesis of SAHs. Modified silica can be used to create highly water-resistant surfaces. The addition of vinyl groups to silica can improve elastic and mechanical properties without significantly changing the density or significantly.

EXPERIMENTAL

Materials and Methods

Sugarcane bagasse, VTMS (vinyltrimethoxysilane), APS (Ammonium Persulfate) as initiator from Merck, SDBS (Sodium Dodecyl Benzene Sulfonate), Ethanol from Merck, Aquadest, HCl 1 M, NaOH 1 M, Ammonium Hydroxide 25%, and Buffer Solution pH 4 and 9.81.

Preparation of Silica Nanoparticles from Sugarcane Bagasse

The bagasse was washed, dried, and cut into small pieces of about 1 cm, then calcined at 650°C for 2 hours. The calcined ash was washed with 10 mL of 1M HCl for 1 grams of ash, then filtered and rinsed with distilled water until neutral. 1 grams of residue was stirred with 8 mL of 1M NaOH at 100°C for 1 hour, then filtered. The sodium silicate solution filtrate was then titrated with 1 M HCl to form aquagel and allowed to stand for 24 hours before being washed and dried. The resulting silica xerogel was crushed using a mortar until it became a fine powder, then sieved with a 200-mesh sieve.

Crosslink Synthesis Stage

Silica nanoparticles were functionalized by mixing VTMS, ethanol, and SDBS (1 g: 15 mL: 100 mL: 0.0126 g), then stirring at 600 rpm for 30 minutes at 25°C. After that, 10 mL of 25% ammonium hydroxide was added and stirred again at 300 rpm for 24 hours. The modified nanoparticles were then centrifuged at 2000 rpm until the solution and solids were separated. The solids in the form of VSNPs were then dried in an oven.

Superabsorbent Hydrogel Synthesis Stage

2.5 grams of NaOH was dissolved in 20 mL of distilled water, then 10 grams of acrylic acid, a crosslinking agent, was added and stirred at 300 rpm at 70°C for 2 hours. Ammonium persulfate as initiator was then added and stirred again for 30 minutes. The formed solution was poured into a petri dish, then dried in an oven at 50-60°C until hydrogels were formed.

Detection Method

Superabsorbent Hydrogel Absorption Capacity Testing

The superabsorbent hydrogel was weighed at 0.01 grams and then immersed in 15 mL of Aquadest. The sample was left to swell for 24 hours at room temperature to allow maximum water absorption. After the absorption period, the unabsorbed liquid was removed. The swollen hydrogel was then weighed to determine its final mass. The absorption capacity was subsequently calculated using the equation below:

$$Q = \frac{w_2 - w_1}{w_1} \cdot 100\%$$

Description: Q = Absorption capacity, W_1 = Weight of the dry sample before soaking, W_2 = Weight after the sample expands.

Swelling Ratio Testing of Superabsorbent Hydrogel in pH 4 and 9.81 Solutions

The superabsorbent hydrogel was weighed at 0.01 grams and then immersed in 10 mL of buffer solution (pH 4 and PH 9.81) and left to swell for 24 hours at room temperature. After the absorption period, the unabsorbed liquid was removed. The swelling ratio of the superabsorbent hydrogel was calculated to evaluate its absorption capacity under varying pH conditions:

$$\text{Swelling Ratio} = \frac{w_2 - w_1}{w_1} \cdot 100\%$$

Description: W_1 = Weight of superabsorbent hydrogel in swelling state, W_2 = Weight of superabsorbent hydrogel in dry state.

Fourier Transform Infrared (FTIR) Testing

The samples were analysed in the form of gels. The type of instrument in Fourier Transform InfraRed (FTIR) testing is the Shimadzu IR-Prestige-21 Series 800 spectrometer model, Japan, with a vulnerable peak of 400 – 4000 cm-[1].

Scanning Electron Microscope (SEM) Testing

Samples were analysed in the form of gels. The type of equipment used in the test Scanning Electron Microscope (SEM) model Thermo Fisher Scientific (FEI), Quanta 6504831403004-AL2-189697044.

X-Ray Diffraction (XRD) Testing

Samples are analysed in the form of dry solids. The type of tool used in X-Ray Difraction testing is MiniFlex 300/600 detector SC-70 with a scan range of 50,000 - 90,000 deg.

RESULTS AND DISCUSSION

This research was conducted to develop a superabsorbent hydrogel that can absorb large amounts of water and has a large swelling ratio in a pH solution. This superabsorbent hydrogel was made by utilizing acrylic acid as a monomer, ammonium persulfate (APS) as an initiator, and Vinyl Silica Nanosphere (VSNPs) as a crosslinking agent. The free radical polymerization technique is used to create superabsorbent hydrogels. The mechanism of free radical polymerization includes three stages: initiation, propagation, and termination.[6] Initiation is the stage where the initiator begins to produce free radicals. APS used as an initiator will decompose to form free radicals when heated. Furthermore, polymer chains will begin to form at the propagation stage. The free radicals formed during the initiation stage will attack the AA monomer molecules to form long polymer chains. The use of acrylic acid as a monomer is regarded as favorable since it can form hydrogels with high water absorption capacities.[7]

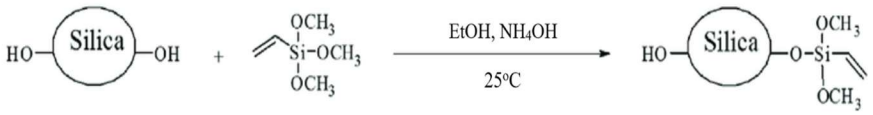

Fig.-1: Nanosilica Modification Reaction Using Vinyl Groups

To form crosslinks between polymer chains, crosslink agents in the form of VSNPs are used. The VSNPs crosslink agent used is the result of modification of VTMS compounds and bagasse nanosilica; the reaction of this modification can be seen in Fig.-1. The usage of VSNPs as a crosslink agent is thought to increase the crystallinity and density of polymer crosslinks, forming a stronger polymer network structure.[8] A strong network structure can make the hydrogel capable of retaining large amounts of water. The last stage is termination, where the growth of the polymer chain is stopped by destroying the active centers of the polymer chain.

Effect of Variation of Initiator and Crosslink Agent on Absorption Capacity Value of Superabsorbent Hydrogel Product

Based on Fig.-2, the hydrogel with the highest absorption capacity is shown in the addition of 0.1 grams APS and 0.1 grams VSNPs, with an absorption capacity of 74,139%. At 0.075 grams and 0.1 grams of initiator, the resulting absorption capacity shows an increase along with the increasing amount of APS added.[9] However, at the addition of 0.125 grams of APS, the absorption capacity showed a decrease. The increase in absorption capacity from 0.075 grams and 0.1 grams APS addition is since at 0.1 grams VSNPs, the number of free radicals generated during the polymerization process increases. During the process of polymer chain formation, free radicals that are essentially devoid of paired electrons will attempt to seek additional electrons by continuously actively attacking the double bonds of AA monomer molecules. When free radicals interact with monomers, monomer radicals are produced, which allows lengthy polymer chains to develop gradually. Long polymer chains will strengthen the polymer network structure.[10]

Based on Fig.-2, the absorption capacity of superabsorbent hydrogel increases with the increase in the amount of VSNPs used, except for the 0.1 grams initiator variation. This is due to the formation of more cross-links between acrylic acid monomers, which in turn increases the number of hydrophilic groups in

the polymer structure. The hydrogel may absorb enormous amounts of water because it has more hydrophilic groups.[11]

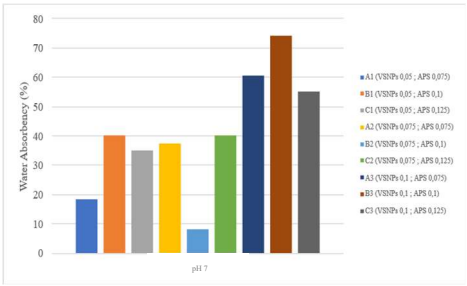

Fig.-2: Effect of VSNPs and APS Amount on Water Absorbency

However, in the B2 variation (0.1 grams of APS and 0.075 grams of VSNPs), the absorption capacity produced was quite low. This is because during the polymerization process, the interaction between APS with monomers and VSNPs seems to be less than optimal. As a result, the structure of the polymer network formed is less than perfect and resulting in a very low absorption capacity.

Effect of Variation of Initiator and Crosslink Agent on Value Swelling of Superabsorbent Hydrogel Products

Based on the results of Fig.-3, the effect of the addition of APS and VSNPs on the swelling value in pH solution is shown. Based on the data analysis conducted, the minimum point is obtained in sample B with a variation of APS 0.1 grams and VSNPs 0.1 grams. The highest swelling value in alkaline atmosphere conditions is pH 9.81 by reaching 31,317% or the weight of the material becomes 4,9011 b/b of the initial material weight of 0.0156 grams. The lower the pH of the solution, the smaller the swelling value. This can indicate that the hydrogel product is difficult to dissolve in acidic conditions (<5).

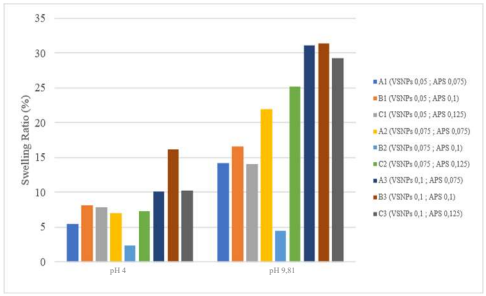

Fig.-3: Relationship between APS and VSNPs Effect on Swelling

The hydrogel product with the highest swelling value was obtained at pH 9.81. This hydrogel product prefers to expand to pH 9.81 due to the influence of the pH of the VSNPs solution. Vinyl Silica Nanaosphere (VSNPs) as a crosslink agent is formed based on two synthesis principles by hydrolysis of VTMS and condensation reactions of silanol bonds under alkaline conditions. Hydrolysis of ethoxyl groups (-OEt) on VTMS into silanol groups (-Si-OH), OH- ions in solution act as a catalyst, accelerating the disconnection of ethoxyl groups from VTMS. After the formation of silanol groups, these molecules then undergo self-condensation, which is the merging of silanol groups into siloxane bonds (Si-O-Si). This process causes the formation of VSNP particles that have a porous structure and a nanoscale.[8] Based on the chemical properties of the main chain (backbone), namely PAA, with compound solution conditions with a pH range of 5. In Poly (Acrylic Acid) or PAA compounds that have carboxylic groups that have many carboxyl groups (-COOH) in the main chain. This group is acidic because it can release H^+ ions in solution. When mixed with a basic solution, hydroxide ions (OH^-) can neutralize the carboxylic acid group, producing carboxylate ions. As a result, PAA turns into an anionic polyelectrolyte (negatively charged chain) that can absorb more water due to electrostatic repulsion between the negatively charged carboxylic groups in the polymer chain. Thus, the swelling ratio under alkaline conditions gives better absorption results than the swelling ratio under acidic conditions.

FTIR Characterization of Sugarcane Bagasse Nanosilica and Superabsorbent Hydrogel Best Sample

The manufacture of VSNPs uses natural raw materials in the form of nanosilica from bagasse ash. The identification stage of functional groups was carried out at wave numbers 500 - 4500 cm^{-1}. The sol-gel approach can identify up to 92.5% of functional groups in the nanosilica polymer of sugarcane bagasse.[12]

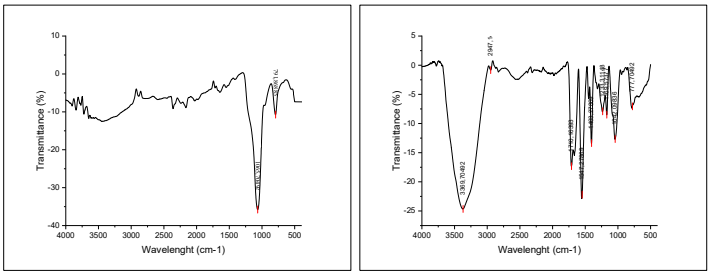

(a) (b)

Fig.-4: FTIR Spectrophotometry of (a) Sugarcane Bagasse Nanosilica; (b) Hydrogel Variation of VSNPs 0.1 grams and APS 0.1 grams

The silica content contained in bagasse ash is organic-type silica, which is an amorphous synthetic compound. Infrared spectrum readings can be seen in Table-1 as follows.

Table-1: FTIR Spectrophotometer Readings of Sugarcane Pulp Nanosilica

Long wave (cm^{-1})	Function Group	Description
791.87	Si-O-Si	Silanol group
1065.70	Si-O-Si	Silanol group

Based on Table-1, the results of reading the FTIR spectrum graph show that there is a silanol group in the nanosilica sample from bagasse ash. The silanol group at wave number 791.87 cm^{-1} is a symmetric stretching of Si-O-Si.[13] The silanol group at wave number 1065.70 cm^{-1} is an internal asymmetric of SiO_4. This shows that the synthesized silica already shows the appropriate bonding characteristics. The material used in the formation of VSNPs is nanosilica, which is indicated by the presence of silanol groups, which can be shown in the absorption peak of 1044.31 cm^{-1}. This absorption peak value is like the strain of silanol groups (Si-O-Si) measured in research.[14] The result of this polymerization process is shown in Fig.-4b, where there is a bond between the polymer chains of PAA, VSNPs, and APS. PAA, which is the main chain (backbone), can be identified alcohol group (-OH) at an absorption peak of 3358.85 cm^{-1}. The amide III group detected at an absorption peak of 1233.31 cm^{-1} confirms the presence of a PAA monomer. This sample contains an amide bend (N-H) group with an absorption peak of 1554.27 cm^{-1}, indicating that not all initiators go through polymerization.[15]

Table-2: FTIR Spectroscopy Readings of Superabsorbent Hydrogel

Long Wave (cm^{-1})	Function Group	Description
777.70	Si-O-Si	Silanol groups that remain react
1042.1	C-O	Carboxyl group from polymerization and Silanol Groups of VSNPs
1169.57	C-O	The carboxyl group from polymerization
1233.31	C–N *stretching*	Amide group III of PAA
1403.65	$C-H_3$	Aromatic groups of the PAA chain
1554.27	N-H bend	The amide group of the APS initiator
1554.27	C=C	Aromatic groups of VSNPs
2947.15	C-H	Aliphatic groups of the PAA chain
3369.70	-OH	Alcohol groups of the PAA chain

The PAA monomer shown in the absorption peak of 1554.27 cm^{-1} is an aromatic group.[16] APS decomposes to produce sulfate radicals (SO_4^-), which then initiate polymerization reactions by attacking double bonds in monomers, shown in the absorption peak of 1403.65 cm^{-1}. This polymerization process also forms aliphatic groups (C-H), which can be seen at the absorption peak 2953.61 cm^{-1}. The results of the final stage of polymerization showed an absorption peak of 1044.31 cm^{-1} and 1169.82 cm^{-1}, which are carboxylic (C-O) functional groups.[17]

X-RD Characterization of Sugarcane Bagasse Nanosilica and Superabsorbent Hydrogels

The functional groups of silica in the nanosilica from bagasse are shown in Fig.-5a. Based on the peaks in the XRD pattern, the broad peaks indicate the amorphous silica phase. The amorphous phase peaks in Fig 6a. are shown at 2θ: 21.76°. The extreme peak indicates the crystalline phase of silica; this peak is shown at 2θ: 31.98°.

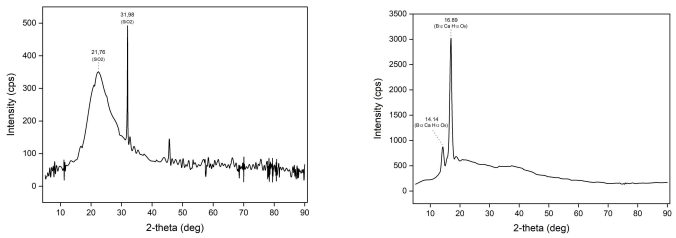

(a) (b)

Fig.-5: XRD Graph of (a) Sugarcane Bagasse Nano-silica; (b) Hydrogel Variation of VSNPs 0.1 grams and APS 0.1 grams

A clearer reading of the X-RD results can be seen in Table-4, as follows.

Table-3: Reading of XRD Graph of Sugarcane Bagasse Ash Nanosilica

2θ	Function Group	Description
21.76°	Si-O-Si	Silanol group
31.98°	Si-O-Si	Silanol group

Based on Table-3. the results of reading the graph show that the resulting silica peaks are located at 2θ: 21.76°, and 31.98°. This is by research, which states that the peak for silica is located between 2θ: 20° - 32°.[18] The crystal structure also resulted from hexagonal X-RD analysis by the lattice a = 4.09 and b = 2.7974. These silica nanoparticles are located at 2θ: 21.76° and 31.98° with a hexagonal shapeAfter crosslinking, the material experiences a phase transition to become denser and stiffer due to the creation of a three-dimensional polymer network that connects the silica nanoparticles.[19] Crystallization in this process leads to the appearance of sharp peaks in the X-ray diffraction (XRD) pattern, which is the result of the crosslinking process, showing an increase in the regularity of the material structure. This strengthens the mechanical properties and stability of the formed material. The XRD pattern of the hydrogel sample is shown in Fig.-5b, the XRD pattern of the dry hydrogel shows a weak peak at 2θ: 16,891°. This hydrogel structure is attributed to the strong intermolecular hydrogen bonding of the acidic molecular chain. The peak at 2θ: 14.14° of the hydrogels bound with VSNPs. The peak shift illustrates that the addition of VSNPs can increase the crystallinity of the hydrogel and increase the crosslinking density of the hydrogel, which will make the hydrogel harder.[20] However, excessive VSNPs content will cause excessive crystallinity of the hydrogel, resulting in a low swelling ratio.[8]

Characterization of Surface Morphology Structure of Sugarcane Bagasse Nanosilica and Superabsorbent Hydrogel by SEM Analysis

Characterization using Scanning Electron Microscope (SEM) aims to show texture, pore size, and irregularities on the surface, making it very important in material analysis. The morphological structure characterization of bagasse nanosilica and superabsorbent hydrogels of the best samples (APS 0.1 grams and VSNPs 0.1 grams) can be seen in Fig.-6 and 7.

This bagasse nanosilica was synthesized using the sol-gel method. The sol-gel method is used because of its ability to form high-purity products.[21] Based on Fig.-6, Nanosilica has an amorphous or uneven surface structure consisting of spherical chunks and indicating that the size of this nanosilica is quite diverse. This amorphous and uneven structure is usually typical of artificially synthesized natural nanosilica materials.[22] Where the amorphous structure is formed is expected because the bonding between particles has not been fully controlled during the synthesis process.[23] The dark areas in the SEM micrographs show that the nanosilica has varying sizes.

The morphological structure of the superabsorbent hydrogel is shown in Fig.-7. The surface morphology at 1000x and 3000x magnification shows that there are complex structures such as long lines, which is an

indication of the crosslinking between monomers, initiator, and crosslinker.[24] But the distribution does not appear to be completely uniform.

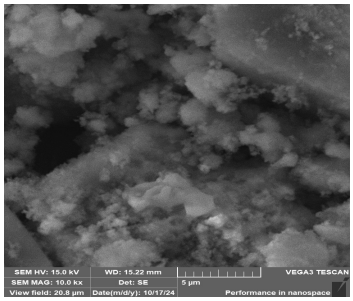

Fig.-6: SEM Micrograph of MAG from Sugarcane Bagasse Nanosilica

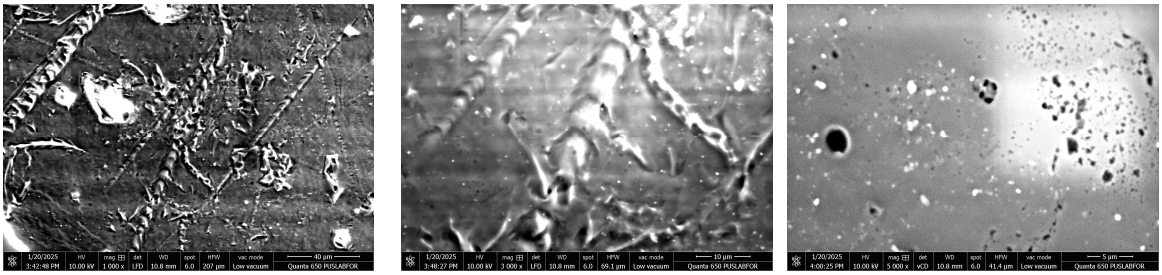

(a) (b) (c)

Fig.-7: SEM Micrograph of Hydrogel Variation of APS (0.1 grams) and VSNPs (0.1 grams), (a) 1000x Magnification; (b) 3000x Magnification; And (c) 5000x Magnification

This apparent non-uniform structure is due to the use of nanosilica-based crosslinkers, where the nanosilica used has an amorphous and heterogeneous structure. The gaps seen at 3000x and 5000x magnification indicate that the resulting hydrogel has pores; the presence of these pores allows for absorption and swelling due to the liquid absorbed in the hydrogel. [25]

CONCLUSION

The superabsorbent hydrogels produced exhibited complex structures characterized such as long lines, which is an indication of the cross-linking between monomers, initiator, and crosslinker. The absorption capacity of these hydrogels increased with the addition of initiator and crosslink agents, reaching an optimum point at the addition of APS and VSNPs, 0.1 grams. The maximum absorption capacity was recorded at 74,139%. The concentration of APS and VSNPs significantly influenced the hydrogel swelling ratio, with the highest absorption occurring in an alkaline pH environment, reaching 31,317%. Nanosilica derived from bagasse demonstrated strong potential as a crosslink agent due to its Si-O-Si functional groups, which interact with polymer chains through hydrogen bonding and silanol condensation. The incorporation of VSNPs as a crosslinking agent is believed to enhance the crystallinity and crosslinking density of the polymer, resulting in a more robust polymer network structure.

CONFLICT OF INTERESTS

The authors declare that there is no conflict of interest.

AUTHOR CONTRIBUTIONS

The present work is related to *SDG-13: Climate Action*. All the authors made significant contributions to this manuscript, actively participated in the reviewing/ editing, and approved the final version for publication. The research profiles can be verified through their ORCID ids, given below:

P. Susmanto https://orcid.org/0000-0003-2219-3782
T. I. Sari https://orcid.org/0000-0001-6426-7482
N. Haryani http://orcid.org/0009-0008-2357-4601
A. Hasanah https://orcid.org/0009-0003-8150-0268
L. Khairunnisa https://orcid.org/0009-0006-8007-0712

REFERENCES

1. I. Meshram, V. Kanade, N. Nandanwar, P. Ingle, *International Journal of Advanced Research in Chemical Science*, **7**, 8(2020), https://doi.org/10.20431/2349-0403.0705002
2. F.Ö. Gökmen, N. Pekel Bayramgil, *Phosphorus, Sulfur, and Silicon and the Related Elements*, **198**, 63(2023), https://doi.org/10.1080/10426507.2022.2113979
3. P. Xu, Z. Shang, M. Yao, X. Li, *Journal of Molecular Liquids*, **357**, 119094(2022), https://doi.org/10.1016/j.molliq.2022.119094
4. P. Chindaprasirt, U. Rattanasak, *Scientific Reports,* **10**, 9890(2020), https://doi.org/10.1038/s41598-020-66885-y
5. M.M. Marin, I.C. Gifu, G.G. Pircalabioru, M. Albu Kaya, R.R. Constantinescu, R.L. Alexa, B. Trica, E. Alexandrescu, C.L. Nistor, C. Petcu, R. Ianchis, *Gels*, **9**, 425(2023), https://doi.org/10.3390/gels9050425
6. G. Irvine, F. Dawson, A. George, M. Kopeć, *European Polymer Journal*, **213**, 113089(2024), https://doi.org/10.1016/j.eurpolymj.2024.113089
7. G. Sennakesavan, M. Mostakhdemin, L.K. Dkhar, A. Seyfoddin, S.J. Fatihhi, *Polymer Degradation and Stability*, **180**, 109308(2020), https://doi.org/10.1016/j.polymdegradstab.2020.109308
8. M. Chen, Y. Shen, L. Xu, G. Xiang, Z. Ni, *Colloids and Surfaces A: Physicochemical and Engineering Aspects*, **613**, 126050(2021), https://doi.org/10.1016/j.colsurfa.2020.126050
9. M.A. Qureshi, N. Nishat, S. Jadoun, M.Z. Ansari, *Carbohydrate Polymer Technologies and Applications*, **1**, 100014(2020), https://doi.org/10.1016/j.carpta.2020.100014
10. M. Tao, S. Lavoie, Z. Suo, M.K. Cameron, *Extreme Mechanics Letters*, **61**, 102024(2023), https://doi.org/10.1016/j.eml.2023.102024
11. A.H. Karoyo, L.D. Wilson, *Materials*, **14**, 1095(2021), https://doi.org/10.3390/ma14051095
12. V. Mamidi, R. Katakojwala, S.V. Mohan, *Biomass Conversion and Biorefinery*, **15**, 4059(2025), https://doi.org/10.1007/s13399-024-05548-8
13. A. Sarker, A.S. Rabbi, N.A. Nadi, A.K.M.L. Rahman, A.A. Momin, K.S. Ahmed, H.A. Simol, *Results in Chemistry*, **11**, 10181(2024), https://doi.org/10.1016/j.rechem.2024.101810
14. R. Ellerbrock, M. Stein, J. Schaller, *Scientific Reports,* **12**, 11708(2022), https://doi.org/10.1038/s41598-022-15882-4
15. N. Özcan, N. Orakdogen, *Gels*, **10**, 556(2024), https://doi.org/10.3390/gels10090556
16. X. Wang, X. He, X. Wang, *Applied Sciences*, **13**, 5162(2023), https://doi.org/10.3390/app13085162
17. M. Al-Kelani, N. Buthelezi, *Skin Research and Technology*, **30**, e13733(2024), https://doi.org/10.1111/srt.13733
18. A. Chauvin, M.-R. Garda, N. Snyder, B. Cui, N. Delpouve, L. Tan, *Journal of Functional Biomaterials*, **15**, 11(2024), https://doi.org/10.3390/jfb15010011
19. A.S. Priya, R. Premanand, I. Ragupathi, V.R. Bhaviripudi, R. Aepuru, K. Kannan, K. Shanmugaraj, *Journal of Composites Science*, **8**, 457(2024), https://doi.org/10.3390/jcs8110457
20. C.W.H. Rajawasam, O.J. Dodo, M.A.S.N. Weerasinghe, I.O. Raji, S. V Wanasinghe, D. Konkolewicz, N. De Alwis Watuthanthrige, *Polymer Chemistry*, **15**, 219(2024), https://doi.org/10.1039/D3PY00914A
21. D. Bokov, A. Turki Jalil, S. Chupradit, W. Suksatan, M. Javed Ansari, I.H. Shewael, G.H. Valiev, E. Kianfar, *Advances in Materials Science and Engineering*, **2021**, 5102014(2021), https://doi.org/10.1155/2021/5102014
22. A. Jyoti, R.K. Singh, N. Kumar, A.K. Aman, M. Kar, *Materials Science and Engineering B*, **263**, 114871(2021), https://doi.org/10.1016/j.mseb.2020.114871
23. J. Kang, X. Yang, Q. Hu, Z. Cai, L.-M. Liu, L. Guo, *Chemical Reviews*, **123**, 8859(2023), https://doi.org/10.1021/acs.chemrev.3c00229
24. D. Miura, Y. Sekine, T. Nankawa, T. Sugita, Y. Oba, K. Hiroi, T. Ohzawa, *Carbohydrate Polymer Technologies and Applications*, **4** 100251(2022), https://doi.org/10.1016/j.carpta.2022.100251
25. R. Wang, C. Cheng, H. Wang, D. Wang, *ChemPhysMater*, **3**, 357(2024), https://doi.org/10.1016/j.chphma.2024.07.006

[RJC-9307/2024]